



Evaluating flood risk management practices and vulnerability mapping in Alawuha watershed (North Wollo Zone, Ethiopia) using GIS and remote sensing

Fisha Semaw^{1,2,3} · Getnet Zeleke¹ · Abel Balew¹

Received: 20 April 2021 / Accepted: 13 March 2022 / Published online: 20 April 2022

© The Author(s), under exclusive licence to Società Italiana di Fotogrammetria e Topografia (SIFET) 2022

Abstract

The current magnitude of flooding in Ethiopia is unprecedented. It is a typical disaster in Ethiopia with the evidence of the recent Dire Dawa and Omo River surroundings, especially during the rainy season. The situation resulted in much human death and destruction of infrastructures in different parts of the country, and the Alawuha watershed is among the typical areas for this problem. The study's aim was to evaluate the flood risk management practices and map flood-vulnerable areas in the Alawuha catchment. Geographic information system (GIS) multi-criteria analysis and remote sensing with field verification were employed to meet the objective of this study. Slope, elevation, rainfall, drainage density, soil type, and distance to rivers are flood event aggravating factors in this study. These factors were weighted accordingly with their contribution to flood hazards. In addition, land use/land cover (LULC) and population distribution were identified as flood vulnerability factors. The weighted overlay analysis result shows that Sanka, Afrikari, Gedo-ber, Hara, and the surroundings, Woldia, were identified as high flood risk areas of the watershed. To minimize this problem, applying physical and biological measures at the watershed level is recommended.

Keywords GIS · Alawuha watershed · Flood risk · Flood hazard · Flood vulnerability

Introduction

Flood is a hydrological condition characterized by high peak discharge that could lead to inundation of lands in adjacent areas, affecting people's lives and livelihoods (Nkeki et al. 2013). Heavy rainfall for long days on the upstream causes most rivers to swell and overflow their courses and sinking the surrounding flat fields (Bhatt et al. 2014). The amount of

rainfall, intensity, and duration in the upstream area causes flooding in down streams. Therefore, floods are related to extreme precipitation and spatial features in the catchments (Boudiaf et al. 2020; Trenberth 2008).

Extensive deforestation and farmland expansion, together with urbanization, raise sensitivity to river peak overflow. Land use changes such as urbanization across the catchment area trigger flood occurrences (Barasa and Perera 2018). This reduction of surface roughness could increase overland flow velocity and floodplain flow rates (Hadjimitsis 2010).

Unpredicted and temporal flash floods are related to rivers in the land areas, where heavy rainfall can change them into destructive torrents within a short period (Obeta and Ochege 2018; Ologunorisa 2004). Since the local climate varies significantly in Ethiopia, flooding incidents also vary in time and space (Desalegn and Mulu 2021; Getahun and Gebre 2015). Flash and river floods are common in Ethiopia during the rainy season between June and September (Akola et al. 2019). Although floods in many parts of Ethiopia are a seasonal phenomenon, the magnitude of the current flooding is unprecedented (Desalegn and Mulu 2021; Bishaw 2012). The recent incident in Dire Dawa city was typical of a flash

✉ Fisha Semaw
semawfisha@gmail.com; ztesawf@gmail.com

Getnet Zeleke
getnetzelke@gmail.com

Abel Balew
abelbalew@gmail.com

¹ Department of Geography and Environmental Studies, Woldia University, Woldia, Ethiopia

² Henan Key Laboratory of Earth System Observation and Modeling, Henan University, Kaifeng 475004, China

³ College of Geography and Environmental Science, Henan University, Kaifeng 475004, China

flood. Furthermore, most flood-related disasters in Ethiopia were attributed to rivers that overflow or burst their banks and inundate downstream plane lands. The situation resulted in many human deaths, displacement, suffering, property loss, and crop damage. The most affected areas are Dire Dawa, South Omo zone of Southern Nations Nationalities and People Region, and parts of Amhara, Oromia, Gambella, Somali, Afar, and Tigray regions (Weldegebriel and Amphune 2017). The Dire Dawa city flood event in 2006 has caused severe direct and indirect damages to social, infrastructure, and economic sectors. The monetary or infrastructural damages also caused 256 people to die, 244 missed, and 15,000 people displaced from their dwellings. This problem is more acute in lowland areas under substantial environmental degradation due to frequent drought. For a large part, this is due to heavy rains falling for long days on the upstream highlands (Alemu and Legesse Belachew 2011; Assegid 2007).

Though flood risk occurrence is a combination of natural and anthropogenic factors, it calls for a better understanding of its spatial extent (Danumah et al. 2016). Flooding is a dynamic process and exhibits spatial characteristics because floods occur at a particular location at which various contributing factors for the event exist (Wu et al. 2018). Flood risk is the product of flood damage and the probability of its occurrence (Dennis Mileti 1999). Therefore, a flood risk map is a crucial information to identify the most vulnerable areas to flooding and estimate the number of people affected by floods in a particular area (Eleni et al. 2011). The extent of flood damage depends not only on the flood characteristics, but also on the inundated site's vulnerability. For the same flood, a more vulnerable area experiences more serious flood damage (De Risi et al. 2020).

The advancement of GIS and remote sensing technologies is enabling scholars to investigate flood hazards and vulnerability. Different remote sensing and GIS approaches have been used to analyze and map flood (Elkhrachy 2015; Ghani et al. 2010; Shaaban et al. 2021; El Bastawesy et al. 2009). Moreover, GIS multi-criteria decision analysis (Feloni et al. 2020), integrated multi-parametric analytic hierarchy process (AHP) and GIS (Ouma and Tateishi 2014), spatial analysis using weighted overlay (Desalegn and Mulu 2021; Rimba et al. 2017), frequency ratio and statistical index (Cao et al. 2016), frequency ratio model (Sarkar and Mondal 2020; Rahmati et al. 2016; Tehrani et al. 2014; Lee et al. 2012), AHP and support vector machine (SVM) (Xiong et al. 2019), and morphometric analysis (Ogarekpe et al. 2020) were used for analyzing and mapping flood hazard, vulnerability, and risk. Other common methods such as artificial neural network (Kia et al. 2012), AHP (Chen et al. 2011), fuzzy analytical hierarchy process (FAHP) (Papaioannou et al. 2015), SVM (Tehrani et al. 2015), and decision tree (Tehrani et al. 2013) were also used for flood investigation.

Several parameters were used by many researchers worldwide to understand and analyze flood hazards and vulnerability and map its risk zone. Factors such as elevation (Desalegn and Mulu 2021; Sarkar and Mondal 2020; Rimba et al. 2017; Cao et al. 2016; Niyongabire et al. 2016; Ouma and Tateishi 2014), aspect (Niyongabire et al. 2016), slope (Desalegn and Mulu, 2021; Sarkar and Mondal 2020; Rimba et al. 2017; Cao et al. 2016; Niyongabire et al. 2016; Elkhrachy 2015; Kazakis et al. 2015; Ouma and Tateishi 2014), LULC (Desalegn and Mulu 2021; Sarkar and Mondal 2020; Barasa and Perera 2018; Rimba et al. 2017; Cao et al. 2016; Elkhrachy 2015; Ouma and Tateishi 2014), soil (Desalegn and Mulu 2021; Sarkar and Mondal 2020; Kusmiyarti et al. 2018; Rimba et al. 2017; Cao et al. 2016; Lincoln et al. 2016; Elkhrachy 2015; Ouma and Tateishi 2014), drainage density (Desalegn and Mulu, 2021; Sarkar and Mondal 2020; Rimba et al. 2017; Elkhrachy 2015; Ouma and Tateishi 2014; Singh and Pandey 2021; Pallard et al. 2009), rainfall (Desalegn and Mulu, 2021; Sarkar and Mondal 2020; Rimba et al. 2017; Kazakis et al. 2015; Ouma and Tateishi 2014), standardized precipitation index (SPI) (Cao et al. 2016), road network (Sarkar and Mondal 2020; Ouma and Tateishi 2014), geology (Cao et al. 2016), surface roughness, distance to river, runoff (Elkhrachy 2015), and population density (Sarkar and Mondal 2020) were used for flood analysis.

The vulnerability to flooding in the North Wollo Zone results from the topography of the district, adjacent districts' watershed direction, the settlement of the households, and poor community management of the watersheds and riverbanks. The climate change-induced excess runoff from these degraded and bare mountainous watershed areas creates powerful erosive forces and hydrodynamic pressures, severely affecting the livelihood of the lowland households. Alawuha river is a persistent river with a significant catchment area (101,988.51 ha). It originates in the western mountainous regions (in the Guba Lafto Woreda) and drains towards Afar Region. An overflow of Alawuha Rivers has a devastating impact on people who live in the watershed. The 2016 flood in the watershed was exceptional because it caused the death of many and the destruction of settlements and infrastructures. Therefore, creating digital terrain maps and flood vulnerability maps of the Alawuha watershed is essential to show the magnitude of flood hazard, vulnerability, and risk zones.

Scholars like Bishaw (2012), Chikoto et al. (2013), and Sena and Michael (2006) conducted a few types of research for flood-related issues in Ethiopia. However, the previous studies did not sufficiently describe the distribution and magnitude of flood-related disasters that happened in the country due to spatiotemporal variation of flooding events. Most of the tasks related to flooding in Ethiopia, specifically in the study area, were based on the administrative boundary. This study aimed to display

how land use and land cover change coupled with climate change causes flooding and its effect on socio-economic and biophysical environments. It is also aimed to identify the practical measures of flood risk assessment and vulnerability mapping using GIS and remote sensing application platforms unlike previous flood studies in Ethiopia that use administrative boundaries as unit of analysis; this study is based on watershed unities. The study investigates each criterion in detail at the micro-watershed level to highlight the minimum flood aggravating factors for watershed management practices. The objectives of this study are (1) to analyze LULC change; (2) to map flood hazard, vulnerability, and risk zones in the Alawuha watershed; and (3) to analyze flood return periods and exceedance probability in the study area. Factors such as LULC, soil type, slope, elevation, drainage density, rainfall distribution, distance to streams, and population density are used as main predictive and determinant factors to map analyze flood vulnerability. The study also used rainfall frequency to estimate exceedance probability of flooding and the possible flooding return periods in the watershed. Even though this study applies multiple criteria and recognized indexes, it's limited in using up-to-date analysis systems like aridity index (AI) and resent machine learning programs. Furthermore, the study will be more accurate and precise through using Copernicus products like sentinel and other open science programs.

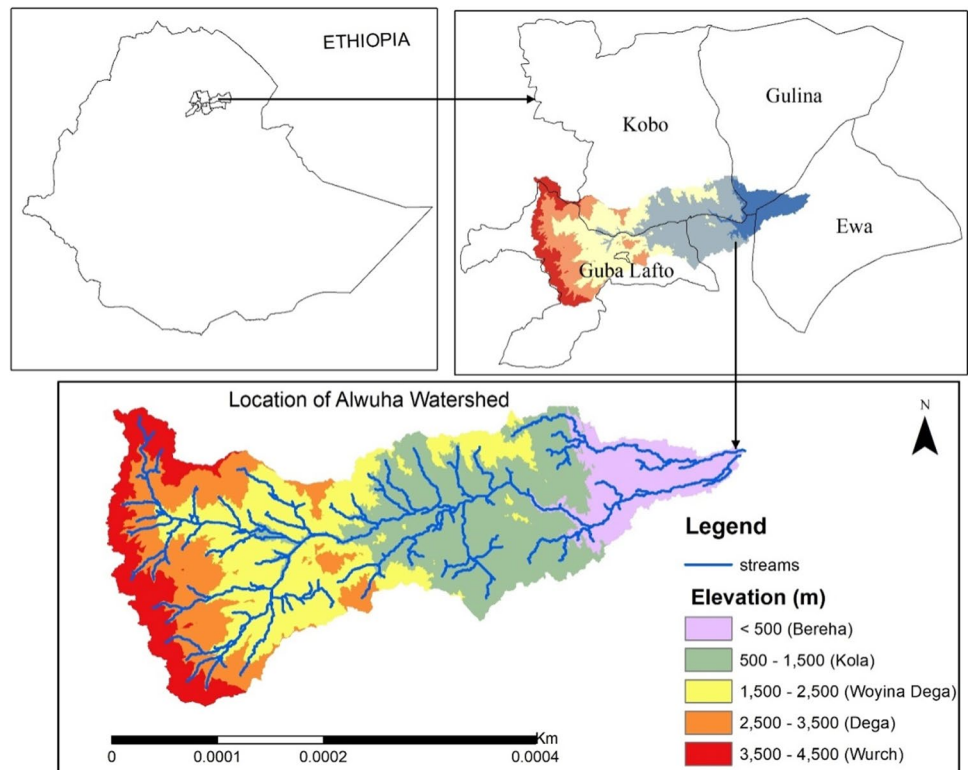
Materials and methods

Description of the study area

Alawuha watershed is geographically located between 10°40' to 12°00' N and 37°40' to 40°00' E (Fig. 1). It has an estimated area of 101,988.51 ha. The altitude of the watershed varies from 800 to 3802 m above mean sea level (amsl).

The area is part of the north-central plateau which is often extensively eroded and dissected by the deep gorges. The eastern boundary of the district is part of the southwestern block of the Afar depression. The elevation varies from 800 to 3200 m in the western plateau to 800 to 1500 m amsl in the low eastern land of the Afar depression. The southeast monsoon and high-elevation westerly's winds are highly influential for the distribution of rainfall; the total annual rainfall is 1000 to 1100 mm year⁻¹ (Loakes et al. 2018). According to the temperature data collected by Sirinka Agriculture Research Center, the mean monthly temperature of the study area ranges between 21 and 25 °C. A bi-modal rainfall is the most dominant in all parts of the watershed. The short rainy season (Belg) occurs between February and May, and the long rainy season (Kiremit) occurs between June and September. In most cases, the highland areas with elevation values vary from 3200 to 3700 m (Dega) which mainly depend on Belg rain. The elevation values range from 1500 to 3200 m (Woyina Dega), and the elevation values vary

Fig. 1 Study area map



from 500 to 1500 m; Kolla areas are rain-dependent from October to January (Meher) for crop production (Mengistie and Kidane 2016; Ali 2002).

Types and sources of data

The study used Landsat images (Landsat 5 TM, 7 ETM+, and 8OLI) to extract LULC types of the watershed. To make the appropriate analysis, Landsat 5 TM 1985, Landsat 7 ETM+ 2000, and Landsat 8 OLI 2016 images were selected. The rationale used for the selection of these periods was due to significant LULC changes resulting from simultaneous occurrences of drought and flood in the study area. Besides, during these three study periods, a significant change of LULC was observed in preliminary survey analysis mainly in 2000 and 2016. Cloud-free Landsat images were downloaded freely from the US Geological Survey (USGS) portal (<http://glovis.usgs.gov>). GPS data were used for training sites, ground verification for image classification, and accuracy assessment control points. A minimum of 30 training sites per class is recommended to classify and validate a satellite image (Congalton and Green 2008). The study used a total of 500 GPS points to validate LULC classification.

Rainfall data from 2000 to 2016 was obtained from the Ethiopian National Metrological Agency (NMA) Kombolcha station. It is used to develop a rainfall distribution map and compute the return period of flooding in the watershed. Furthermore, digital elevation model (DEM) with the 30-m horizontal resolution was obtained from the USGS webpage (<http://glovis.usgs.gov>). The DEM data is used to extract elevation, slope, drainage density, flow direction, stream network, flow accumulation, and watershed map of the study area. The soil data obtained from the Amhara Regional Agricultural Office at a scale of 1:20,000 was also used for flood analysis since it affects the hydrological characteristics. The study area population was obtained from the Central

Statistics Agency (CSA), Ethiopia, to develop a flood vulnerability map since it is one of the affected elements by the flood.

Parameter selection

LULC, soil type, elevation, slope, drainage density, rainfall distribution and frequency (amount), distance to streams, and population density parameters were selected to investigate flood hazard, vulnerability, and risk in the study watershed. These parameters were selected according to the literature presented in Table 1 and the nature of the study area and available data.

Flood factor development

Image classification

The study employed digital image processing techniques such as an atmospheric correction to improve the quality of the images and sub-setting to extract images of the study area. A maximum likelihood supervised algorithm was used to classify the Landsat images. During classification, forest, built-up area, agricultural land, bare land, and riverbank were identified carefully with intensive field observation using local indigenous knowledge to easily interpret and reduce the effects of spatial autocorrelation and redundancy. A confusion matrix was used to validate the image classification and accuracy assessment report for overall accuracy and kappa statistics extracted from the matrix. The images were processed and interpreted in ERDAS Imagine 2015 environment. The LULC type is one of the main factors (Desalegn and Mulu 2021; Sarkar and Mondal 2020; Barasa and Perera 2018; Cao et al. 2016) which is considered in this study because flood vulnerability varies with the variation of surface type and disaster does not equal damage.

Table 1 Parameters used for the study

Parameters	References
LULC	Desalegn & Mulu (2021); Sarkar & Mondal (2020), Barasa and Perera (2018); Rimba et al. (2017); Cao et al. (2016); Elkhachy (2015); Ouma and Tateishi (2014)
Soil type	Desalegn & Mulu (2021); Sarkar & Mondal (2020); Kusmiyarti et al. (2018); Rimba et al. (2017); Lincoln et al. (2016); Elkhachy (2015); Ouma and Tateishi (2014)
Elevation	Desalegn & Mulu (2021); Sarkar & Mondal (2020); Rimba et al. (2017); Cao et al. (2016); Niyongabire et al. (2016); Elkhachy (2015); Ouma and Tateishi (2014)
Slope	Desalegn & Mulu (2021); Sarkar & Mondal (2020); Rimba et al. (2017); Cao et al. (2016); Niyongabire et al. (2016); Kazakis et al. (2015)
Drainage density	Desalegn & Mulu (2021); Sarkar & Mondal (2020); Rimba et al. (2017); Elkhachy (2015); Ouma and Tateishi (2014)
Rainfall	Desalegn & Mulu (2021); Sarkar & Mondal (2020); Rimba et al. (2017); Elkhachy (2015); Kazakis et al. (2015); Ouma and Tateishi (2014);
Population density	Sarkar & Mondal (2020)
Distance to streams	Elkhachy (2015)

Surface analysis

The study used surface analysis to extract slope and elevation thematic layers from DEM using ArcGIS 10.5. The DEM data were preprocessed to remove errors such as sink from the data and enhance its quality. Therefore, fill analysis was applied to fill a hole in the DEM data. The DEM is the most common source of data for elevation and slope (Desalegn and Mulu 2021; Sarkar and Mondal 2020; Rimba et al. 2017; Niyongabire et al. 2016).

Hydrological analysis

Flow direction, flow accumulation, stream network, drainage density, and watershed were developed using hydrological analysis (Desalegn and Mulu 2021; Sarkar and Mondal 2020; Rimba et al. 2017; Elkhrachy 2015). Watershed delineation analysis was done to extract streams from DEM-based watershed snap pour points. The DEM is used as an input

rater to extract surface elevation raster (fill DEM). Flow direction raster was extracted from surface raster, and flow accumulation was extracted from flow direction. Stream raster was created from flow accumulation using a conditional standard query language (SQL) in the Raster Calculator tool. The Strahler stream ordering method from raster and flow direction was employed to create stream order (Fig. 2). Then, snap pour points were digitized to identify river outlets. Using digitized snap pour points and flow accumulation, snap pour raster was created. Then, from flow direction and snap pour raster, the watershed was delineated and converted to polygon (Fig. 3). Finally, a buffer analysis was applied in ArcGIS 10.5 to extract the distance of the stream layer. Distance from stream channel is the basic element in flood hazard mapping because the peak flow of the river largely damages the surrounding area of the river.

Drainage density is the ratio of the total length of all the rivers and streams in a watershed in km and the total surface area of a watershed in km² (Darama and Seyrek 2016;

Fig. 2 Stream network extraction model

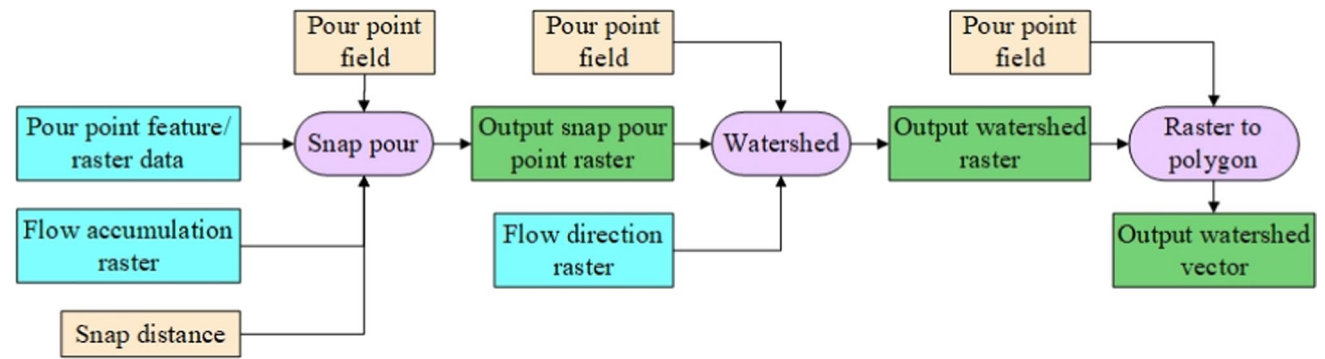
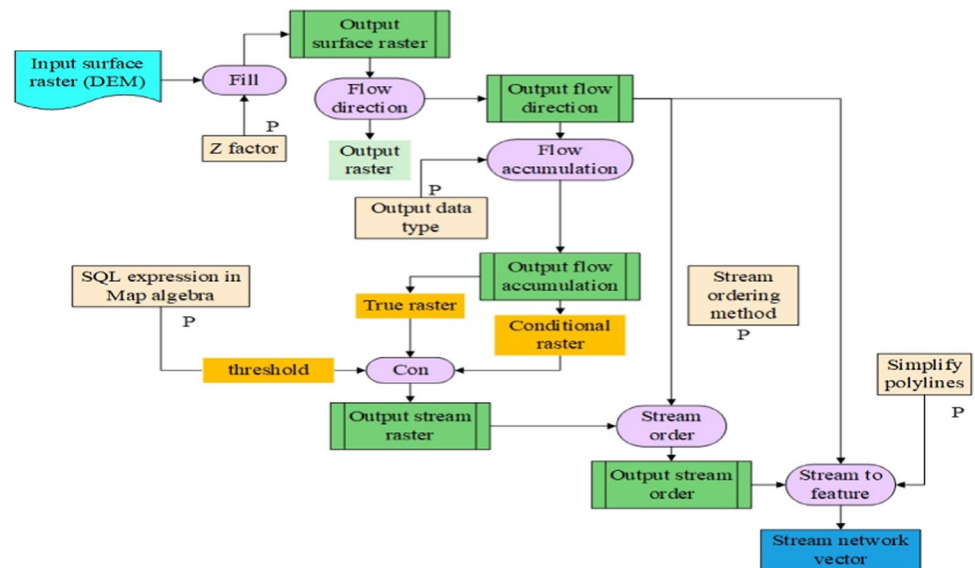


Fig. 3 Watershed delineation model

Horton 1945). Watershed with high drainage density indicates that more precipitation quickly joins streams whereas low density means more precipitation traveled as surface runoff, through flow and baseflow. The drainage density determines water outlets and rock structures. The drainage density analysis provides a numerical measurement of landscape dissection and runoff potential. It can be calculated using Eq. (1):

$$DD = \frac{\sum L_s}{A_w} \quad (1)$$

where DD is the drainage density, L_s is the length of streams, and A_w is the area of watershed.

Surface interpolation

The study employed inverse weight distance (IDW) surface interpolation to develop rainfall distribution thematic layer of the Alawuha watershed from rainfall frequency data. Rainfall distribution was considered as a layer for flood vulnerability analysis because it shows the possible surface runoff water in the area. It is used by some previous studies (Desalegn and Mulu 2021; Sarkar and Mondal 2020; Rimba et al. 2017; Elkhachy 2015; Kazakis et al. 2015; Ouma and Tateishi 2014).

Population density analysis

Population density layer was also used for flood vulnerability parameter (Sarkar and Mondal 2020) because flood hazard and its vulnerability are very severing in the area of settlement than other open environment. Population density factor was extracted using kernel density analysis in ArcGIS environment since the kernel density is a common nonparametric estimator of variety of variable (Kim and Scott 2012).

Soil types

Haplic Xerosols, Chromic Cambisols, Euthric Cambisols, Vertic Cambisols, Chromic Vertisols, Euthric Regosols, Calcic Flubisols, Leptosols, and Phaeozems are main the soil types found in the watershed. These soil types were extracted with the watershed boundary and then classified into five classes to evaluate soil susceptibility to flooding. Soil type is also taken as a factor for flood analysis (Desalegn and Mulu 2021; Sarkar and Mondal 2020; Kusmiyarti et al. 2018; Rimba et al. 2017; Lincoln et al. 2016) because it influences the magnitude and direction of flooding.

All layers were standardized to create uniform thematic layers for overlay analysis. Standardized layers were developed based on the literature, expert's knowledge, the nature of the topography, and the data of the study. Equal weight

influence was used to create a final flood hazard map of the watershed since no specific measures are taken to minimize their effect on flooding. In evaluating parameters, sub-criteria were ranked from 1 to 5, where 1, 2, 3, 4, and 5 represent very high, high, moderate, low, and very low respectively (Table 2).

Flood analysis

Hazard

A flood hazard is a characteristic occasion that may cause a death toll, injury, or other wellbeing impacts, property harm, loss of people and administrations, social and financial disruptions, or natural harm (ISDR, U. N. 2009). Flood hazard is the function of factors that cause flooding in the watershed such as slope, elevation, soil type, and distance to rivers, drainage density, and rainfall distribution. These factors were standardized to five classes as shown in Table 2. Multi-criteria evaluation (MCE) methods were employed to integrate these datasets to produce a flood hazard map. According to Saini and Kaushik (2012), GIS allows multi-criteria evaluation that the decision-makers use to identify a predefined set of criteria with the overlay process. The flood hazard map can be calculated using the following formula adopted from Kazakis et al. (2015):

$$FH = \sum_{i=1}^n ri.wi = S.ws + E.wE + L.wl + R.wr + So.wso + D.wd \quad (2)$$

where $FH = Flood\ Hazard$; ri = the rank of the parameter in each point; wi = the weight of each parameter; n = the number of the criteria; $S.ws$ = soil and weight of soil; $E.wE$ = elevation and weight of elevation; $L.wl$ = land use and weight of land use; $R.wr$ = rainfall and its weight; $So.wso$ = soil and its weight; and $D.wd$ = drainage density and weight.

Multi-factor analyses were performed by using the multi-criteria ranking method to produce the final flood hazard map. Each parameter was ranked and weighted according to the estimated significance for causing flooding and created the final hazard factors map. The weighted overlay result flood hazard map was reclassified into very high, high, moderate, low, and very low.

Vulnerability

The attributes and conditions of a local area, framework, or resource make it defenseless to the harmful impacts of a flood (ISDR, U. N., 2009). Population distribution and LULC thematic layers were used to develop flood vulnerability map of the watershed. A GIS overlay analysis technique was employed in the ArcGIS 10.5 environment to combine the two exposed thematic layers of the study

Table 2 Flood hazard parameters and weights

Parameters	Weight (%)	Sub-class of parameters	Level
Slope	16.67	< 1%	1
		1–3%	2
		3–4%	3
		4–5%	4
		> 5%	5
Elevation	16.67	< 1000 m	1
		1001–1500 m	2
		1501–2000 m	3
		2001–2500 m	4
		> 2500 m	5
Drainage density	16.67	> 0.68 km/km ²	1
		0.54–0.68 km/km ²	2
		0.35–0.54 km/km ²	3
		0.19–0.35 km/km ²	4
		< 0.19 km/km ²	5
Rainfall	16.67	> 1200 mm/year	1
		900–1200 mm/year	2
		700–900 mm/year	3
		500–700 mm/year	4
		< 500 mm/year	5
Soil type	16.67	Haplic Xerosols, Chromic Cambisols, Euthric Cambisols, and Vertic Cambisols	1
		Chromic Vertisols and Euthric Regosols	2
		Calcaric Flubisols	3
		Leptosols	4
		Phaeozems	5
Distance to streams	16.67	< 100 m	1
		100–150 m	2
		150–200 m	3
		200–250 m	4
		> 250 m	5

area. The result of the flood vulnerability map was reclassified into very high, high, moderate, low, and very low.

Risk

Flood risk is the blend of the likelihood of an occasion and its adverse results (ISDR, U. N. 2009). A GIS overlay analysis was employed in the ArcGIS 10.5 Raster calculator tool to create a flood risk map of the watershed. A flood risk map is a composite map that developed from flood hazard and vulnerability maps. It can be computed using Eq. 3:

$$\text{Flood risk} = \text{Hazard} * \text{Vulnerability} \tag{3}$$

Finally, flood risk map was classified into very high, high, moderate, low, and very low risk zones.

Rainfall frequency analysis

Rainfall frequency analysis becomes the most appropriate technique for flood managers to describe floods and identify the extreme events. We used the plotting position rank method to build the relationship between the probability of occurrence or return period of certain events and their magnitude. The ranking method with the Weibull formula plotting position is done by ranking from largest to smallest (Zachariev 2016; Weibull 1939). Hence, the largest observation is assigned plotting position $1/n$ and the smallest $n/n = 1$ for its annual exceedance probability, AEP. The return period, T , of an event, is then the inverse of the AEP. The Weibull formula is stated in Eqs. (4) and (5):

$$AEP = \frac{i}{n + 1} \tag{4}$$

$$T = \frac{n+1}{i} \quad (5)$$

where AEP = annual exceedance probability; T = the return period of an event or frequency; i = rank of an events; and n = the number of considered events.

Results

Land use/land cover change for the period 1985–2016

The land use/land cover of the watershed was classified into five classes, namely, agricultural land, forest land, bare land, built-up area, and riverbed for the years 1985, 2000, and 2016 (Fig. 4a–c), and the area for each LULC classes presented (Table 3). In 1985, the majority of the watershed (44.5%) was categorized as forest land, whereas agricultural

land, riverbed, built-up land, and bare land covered 26.29, 16.38, 9.74, and 3.07%, respectively. For the year 2000, agricultural land accounted for 29.61% of the watershed, whereas bare land, forestland, riverbed, and built-up areas covered 18.54, 17.97, 17.92, and 15.96%, respectively. In 2016 agricultural lands covered 34.14% of the watershed, whereas built-up areas, riverbed, forest land, and bare land covered 21.72, 21.59, 19.19, and 3.36%, respectively.

Net LULC classes' area changes due to natural and anthropogenic factors for the periods 1985 to 2000, 2000 to 2016, and 1985 to 2016 which were presented in Table 3. Between the years 1985 to 2000, forest area showed decreasing trend by 26.55%, whereas the bare land class and built-up areas increased by 15.47 and 6.22%, respectively. Agricultural land and riverbed also show an increase of 3.32 and 1.54%, respectively. In a similar analysis for the period 1985 to 2016, a significant change in either direction for all land use categories was observed. From 1985 to 2016, forest area decreased by

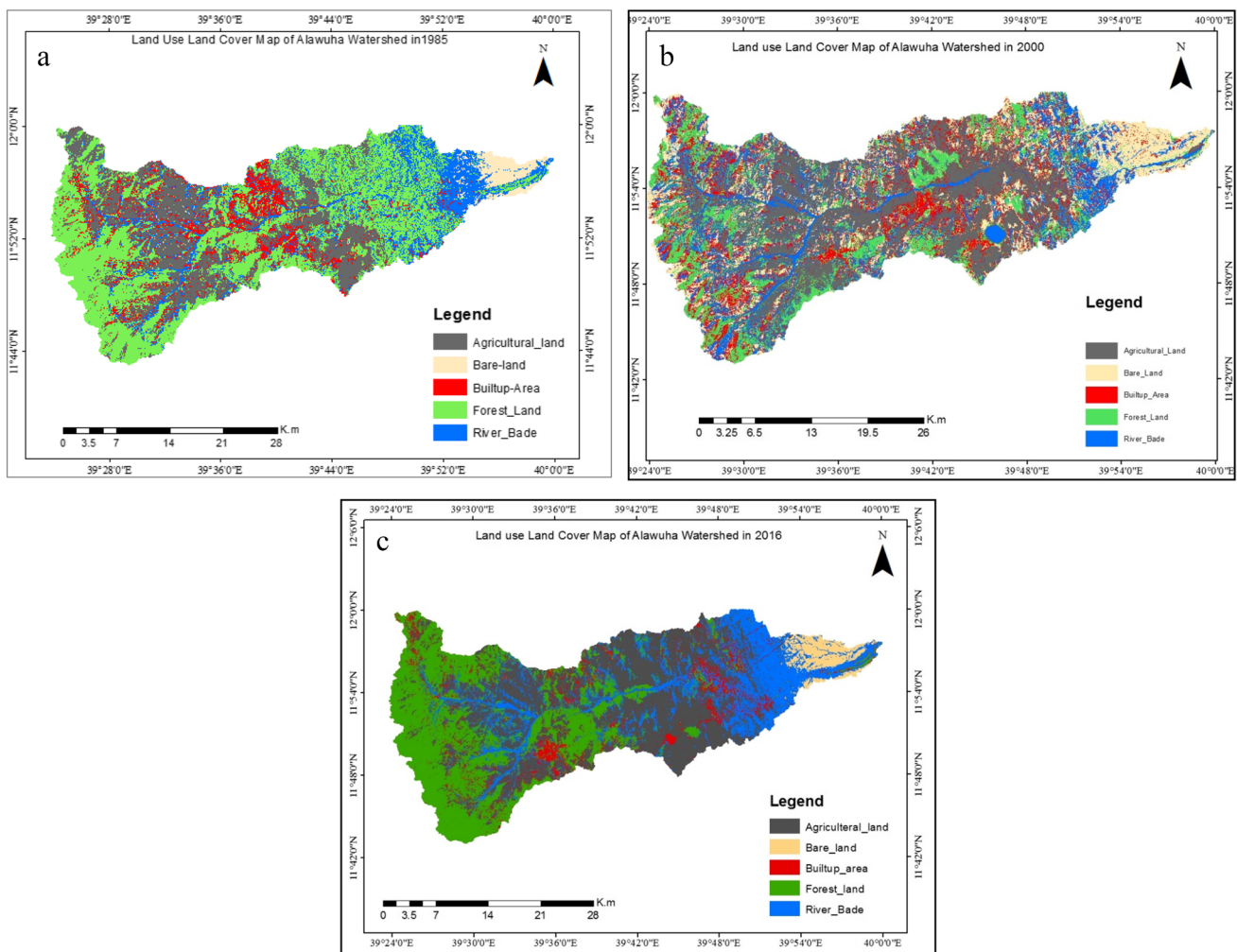


Fig. 4 LULC maps of the watershed from 1985 (a), 2000 (b), and 2016 (c)

Table 3 Trend of LULC changes from 1985 to 2016

Land use class	1985		2000		2016		Change					
	Area (ha)	%	Area (ha)	%	Area (ha)	%	1985–2000		2000–2016		1985–2016	
							(ha)	%	(ha)	%	(ha)	%
Agricultural land	26,821.15	26.29	30,199.68	29.61	34,815.41	34.14	3378.53	3.32	4615.73	4.52	7994.26	7.84
Bare land	3133.38	3.07	18,909.53	18.54	3427.81	3.36	15,776.2	15.47	–15,481.72	–15.17	294.43	0.3
Built-up area	9931.6	9.74	16,281.54	15.96	22,153.2	21.72	6349.94	6.22	5871.66	5.76	12,221.6	11.98
Forest land	45,409.69	44.52	18,323.17	17.97	19,568.62	19.19	–27,087	–26.55	1245.45	1.22	–25,841.1	–25.34
Riverbed	16,692.69	16.38	18,274.61	17.92	22,023.47	21.59	1581.92	1.54	3748.86	3.67	5330.78	5.21

Table 4 Accuracy report of LULC for 1985, 2000, and 2016

Year	1985	2000	2016
Overall accuracy	83.25	85.13	91
Kappa statistics	0.825	0.843	0.901

25.34% primarily due to the expansion of settlement and agricultural land, which increased by 11.98 and 7.84%, respectively. Riverbed and bare lands also showed a significant increase of 5.21 and 0.3%, respectively. Generally, the result has indicated a series of LULC change for the last 30 years (1985–2016). In this regard, the trend has shown more land being used for agriculture and built-up areas. Except for forest land, all other land use categories show expansion for the past 30 years in the watershed and which can cause ecosystem imbalance.

The overall accuracy and kappa statistics of the LULC classification for 1985, 2000, and 2016 were 83.25% and 0.825, 85.13% and 0.843, and 91% and 0.901, respectively (Table 4).

Flood hazard factor analysis

Flood hazard aggravating factors considered in this study include elevation, slope, drainage density, soil type, proximity to the river, and rainfall distribution for the hazard analysis. Understanding the factors which aggravate flooding is significant to watershed conservation and management practices. These flood aggravating factors of the catchment are analyzed as follows.

Slope and elevation

The lower value of the slope is a flatter terrain, and the higher value of the hill is steeper terrain. Based on their susceptibility to flooding, slope and elevation have been classified into five classes. The result indicates that area less than 1000 m in height was very highly susceptible

to flood. Places found in elevation between 1001–1500, 1501–2000, 2001–2500, and > 2501 m were high, moderate, low, and very low sensitivity levels to flood, respectively. Therefore, the result of the study revealed that flood hazard more affects the lowland areas than the highlands. The study also shows that places found in the lowland and smooth surface of downstream of the watershed were very high sensitivity levels of flooding. Such places in the study area have a slope value of less than 1% slope. On the other hand, places found in slope values between 1–3, 3–4, 4–5, and > 5% were highly, moderately, low, and very low affected by flood hazard, respectively (Fig. 5).

Soil type

Nine main soil classes were identified in the watershed based on the soil erosion grouping system (Nachtergaele et al., 2010). These are Chromic Vertisols, Chromic Cambisols, Euthric Cambisols, Euthric Regosols, Calcaric Flubisols, Haplic Xerosols, Leptosols, Phaeozems, and Vertic Cambisols. According to their flood generating capacity, these nine soil types were grouped into five classes. Based on the degree to cause a flood, soils were categorized as very high, high, moderate, low, and very low. Finally, Haplic Xerosols, Chromic Cambisols, Euthric Cambisols, and Vertic Cambisols are categorized as a very high flooding capacity, Chromic Vertisols and Euthric Regosols are categorized as high, Calcaric Flubisols are classified as moderate, Leptosols are classed as a low, and the last Phaeozems are categorized as very low flood generating capacity (Fig. 6).

Rainfall and drainage density

The average rainfall distribution map of the study area was classified into five classes. The study shows that areas that receive with higher rainfall amount annually (> 1200 mm/year) were categorized under “very highly” affected by flood hazard and places that obtain rainfall vary from 900

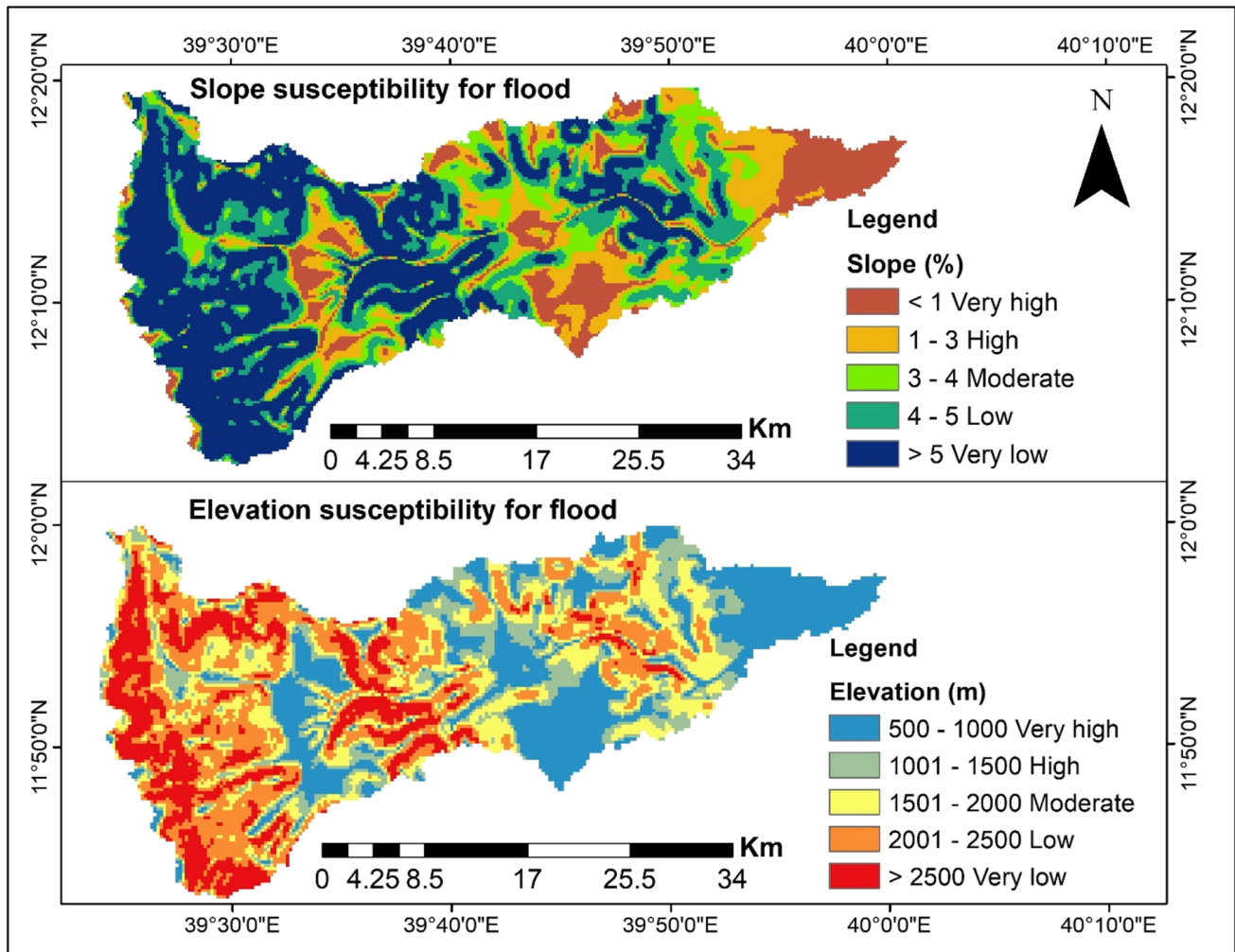


Fig. 5 Slope and elevation flood susceptibility map

to 1200 mm/year highly affected by flood hazards. The study also stated that places receive rainfall between 700–900, 500–700, and < 500 mm/year were found in moderate, low, and very low flood hazard zone, respectively, as shown in Fig. 7.

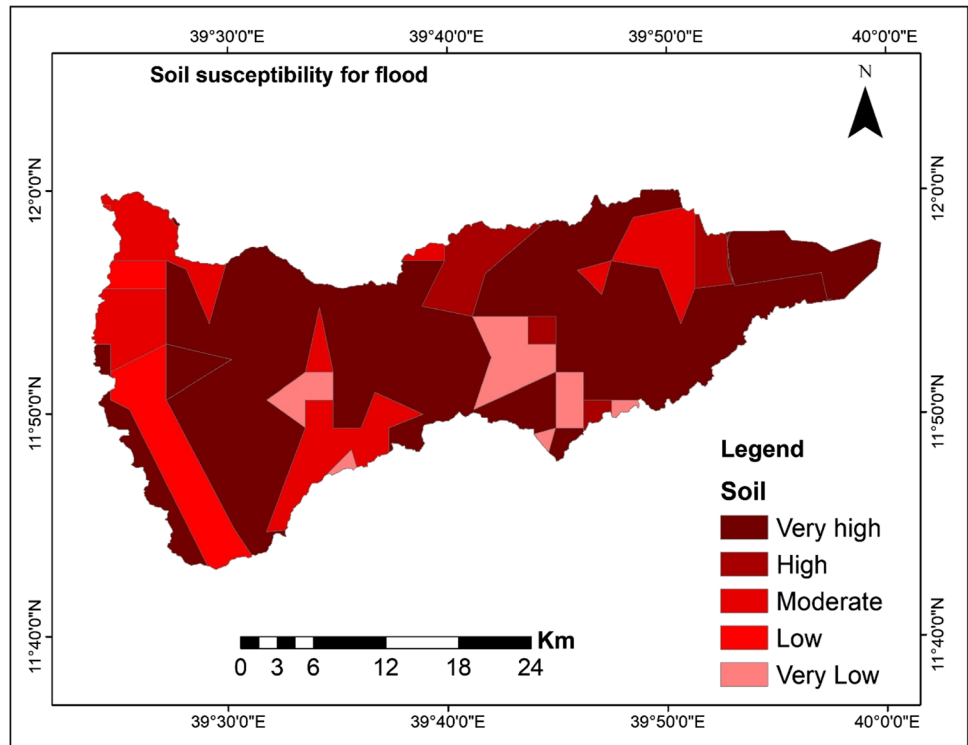
The drainage density of the catchment is used for calculating the volume of the flood in a given stream. However, all the valleys do not necessarily carry water permanently; rather, they are filled by seasonal flooding. The drainage density thematic layer was classified into five classes. The result of this study indicates that areas with a higher drainage density (> 0.68 km/km²) were found in a very high flood hazard zone, while drainage density varies from 0.54 to 0.68 km/km² lay in the high flood hazard zone. Moreover, the drainage density varies from 0.35 to 0.54, 0.19 to 0.35, and less than 0.19 km/km², and places found in these densities were moderate, low, and very low affected by flood hazard, respectively.

Distance to streams

Analysis of distance to streams shows that areas within 100 m distance from streams were very highly exposed to flood hazards. Places found between 100 and 150 m distances from the streams were highly exposed, while the stream distance between 150 and 200 m caused moderate flood hazard. Besides, places lay between the distance of the streams 200–250 and > 250 m were found in low and very low flood hazards, respectively (Fig. 8).

The GIS weighted overlay analysis result of flood hazard factors shows that 12,773.13 ha of the watershed was a very high (dark blue color) flood hazard zone, while 16,644.69 ha was a highly (light blue) hazard zone. Besides, moderate (light purple), low (olive), and very low (green) flood hazard zones have covered an area of 32,211.49, 24,468.58, and 15,731.78 ha, respectively (Fig. 9).

Fig. 6 Soil flood susceptibility map



Flood vulnerability factor analysis

Population distribution and LULC

According to the North Wollo Zone agricultural office, the total household living in the catchment was 197,410. From those households, based on their location, economic activity, property damage (lose), livestock loss, and injured, about 9440 households were affected by the flooding. The result of the study indicates that 8652 in Woldia town, 181 in Guba Lafto Woreda, 162 in Habiru Woreda, 143 in Gidan woreda, 132 in Raya kobo woreda, 120 in Dawint woreda, 35 in Ewa woreda, and 15 households in Gulina woreda will be affected. The result of the study also shows that agricultural land and built-up areas were very high and high vulnerable to flood whereas riverbed, bare land, and forest cover were moderate, low, and very low vulnerable to flood, respectively (Fig. 10).

The result of regression statistics confirmed that the agricultural land and flood vulnerability have a strong positive correlation with a confidence level of 94% and *p* value of 0.06 (Table 5). The correlation of the dependent (flood vulnerability) and independent (agriculture land) variable was 0.96. Built-up and flood vulnerability also have a significant positive correlation with *R*² of 0.93 with the confidence level of 91% and *p* value of 0.09 (Table 6).

The result of the final flood vulnerability analysis indicates that 41,824.12, 17,809.22, 33,042.88, 8815.14, and

497.5 ha of Alawuha watershed were very high, high, moderate, low, and very low vulnerable to flood, respectively. Figure 11 indicates that flame red and orange colors represent very high and high flood-vulnerable area, respectively. Moreover, light green, green, and dark blue colors show moderate, low, and very low flood-vulnerable zones, respectively.

Flood risk analysis

Flood risk is a composite map of flood vulnerability and hazard which indicates the possible impacts that happened due to flood hazards. The final composite flood risk map shown in Fig. 12 indicates that 42,035.66, 22,575.09, 35,658.63, 691.38, and 1027.74 ha of Alawuha watershed was very high, high, moderate, low, and very low to flood risk, respectively. As shown in Fig. 12, red, yellow, olivenite green, light blue, and dark green colors represent very high, high, moderate, low, and very low flood risk zones, respectively. The study revealed that Sanka, Afrikari, and Gedo-ber, Woldia town, Alawuha agricultural land, and the low-lying area of Gulina and Ewa are highly flooded risk areas.

Rainfall frequency

Flood frequency analysis is one of the important studies of flood risk analysis. It is essential to interpret the record of flood events and the amount of precipitation to predict

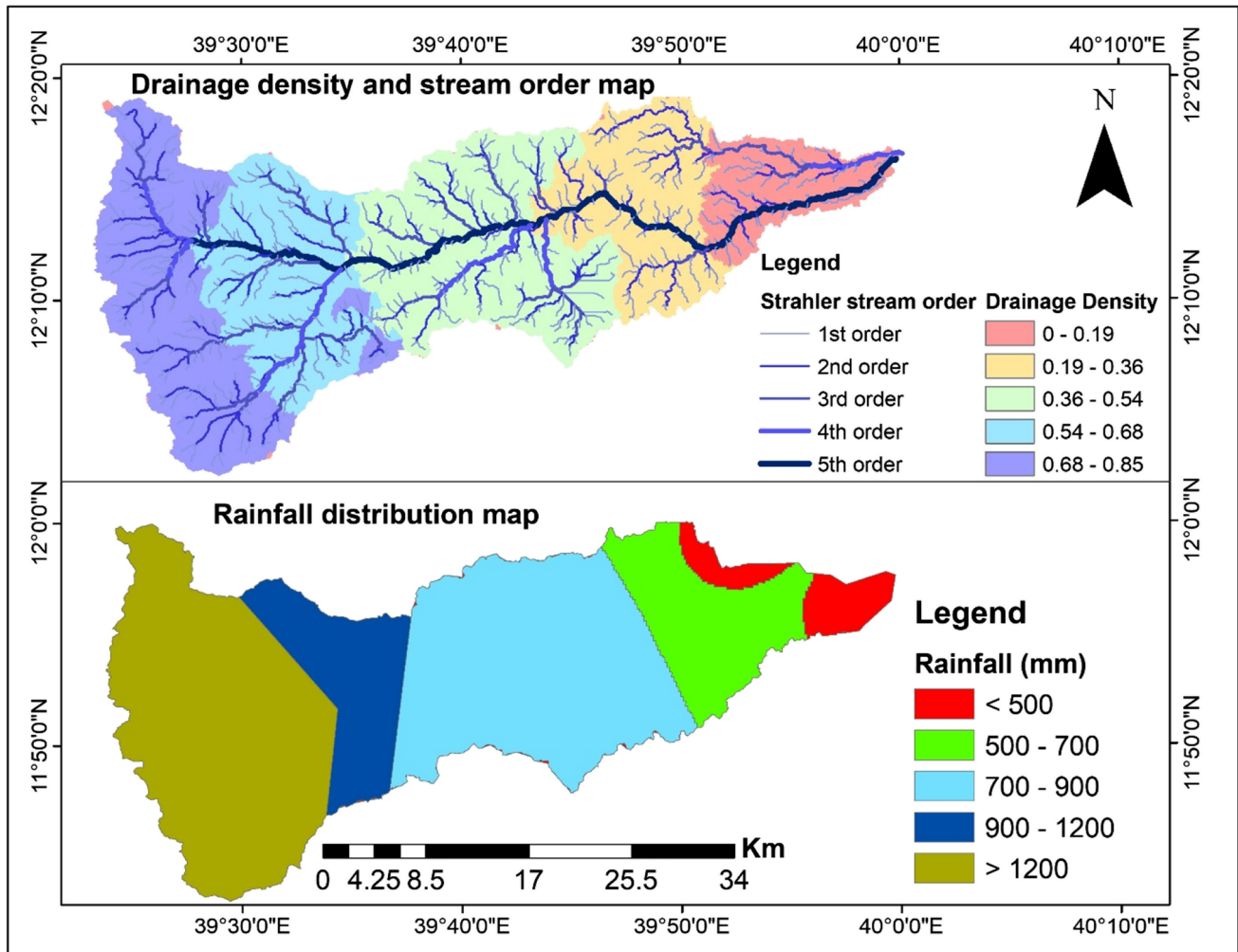


Fig. 7 Drainage density and rainfall hazard map

future possibilities of flood occurrences. It helps to determine the return levels of extreme rainfall and to understand how often such rare events might occur in the future. Frequency analysis result of the watershed indicates that the highest rainfall amount (356.4 mm) was observed in 2016 with the return period of 18 years and annual probability exceedance of 0.05 or 5% (Table 7). The amount of rainfall recorded in 2000 was 260.7 mm, and it has an exceedance probability of 7.14 and the return period of 0.14 years.

Discussion

LULC change and flood

The result of this investigation revealed that built-up, agriculture, and riverbed areas had been increased drastically from 2000 to 2016. Such rapid change of land use/land

cover increases flood occurrence in the study area. Particularly, uncontrolled urbanization and extensive agricultural land expansion bring a dramatic change of landscape patterns and types (Li et al. 2018; Jiang and Tian 2010; Fan et al. 2009); this has a powerful effect on floods. Large areas of the watershed are deforested or drained, increasing or decreasing antecedent soil moisture and triggering erosion. Furthermore, an extreme expansion of urban areas and impermeable surfaces such as asphalt and concrete contribute to the change of river morphology and slope instability. Drains and sewers take water directly to the river, which also increases flood risk. Therefore, managing the land use/land cover is a very significant component of mitigating the impact of flood disasters (Barasa and Perera 2018; Getahun and Gebre 2015). Moreover, the current study stated that urban area (built-up) was the most vulnerable land use class to flood because it is the area where most of the people lived, economic interaction processed, and basis of financial mobility. Thus, the finding

Fig. 8 Distance to stream map

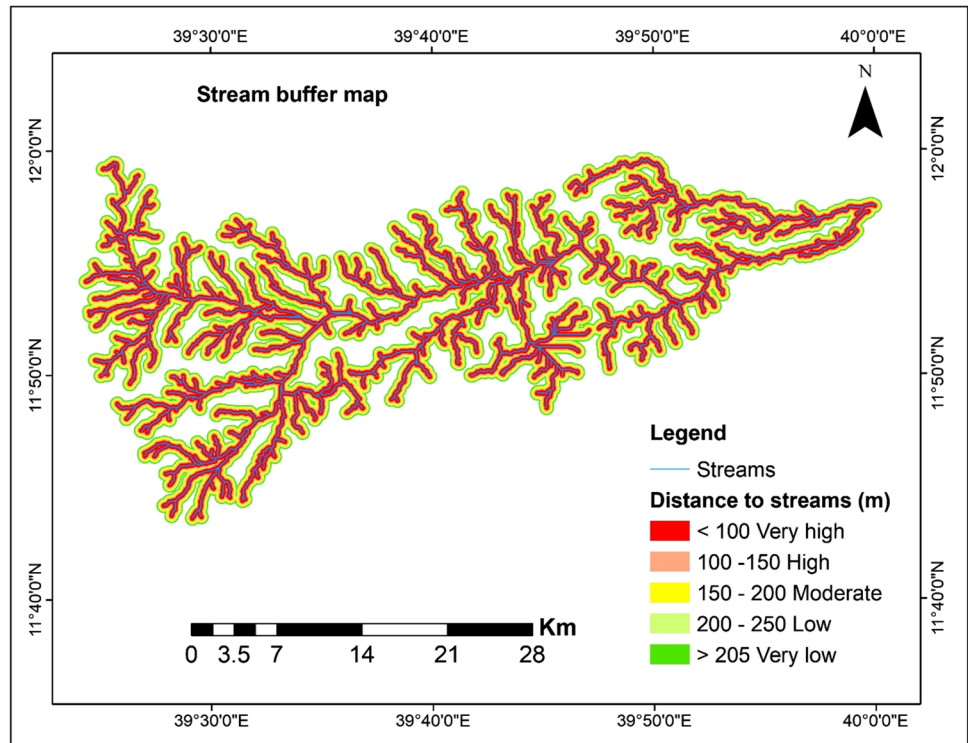
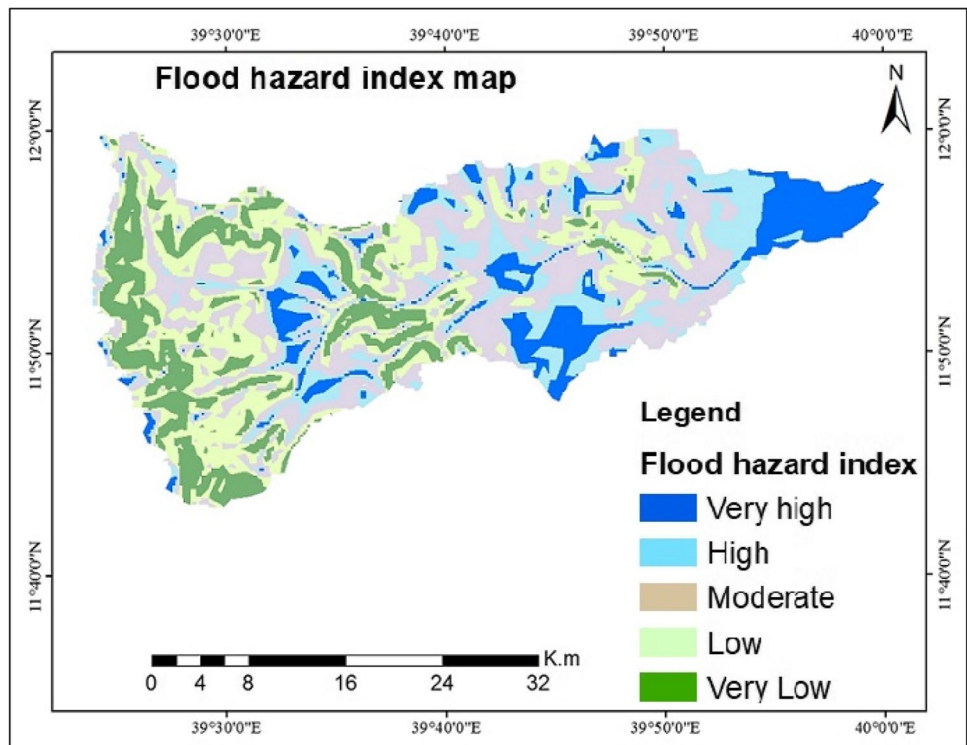


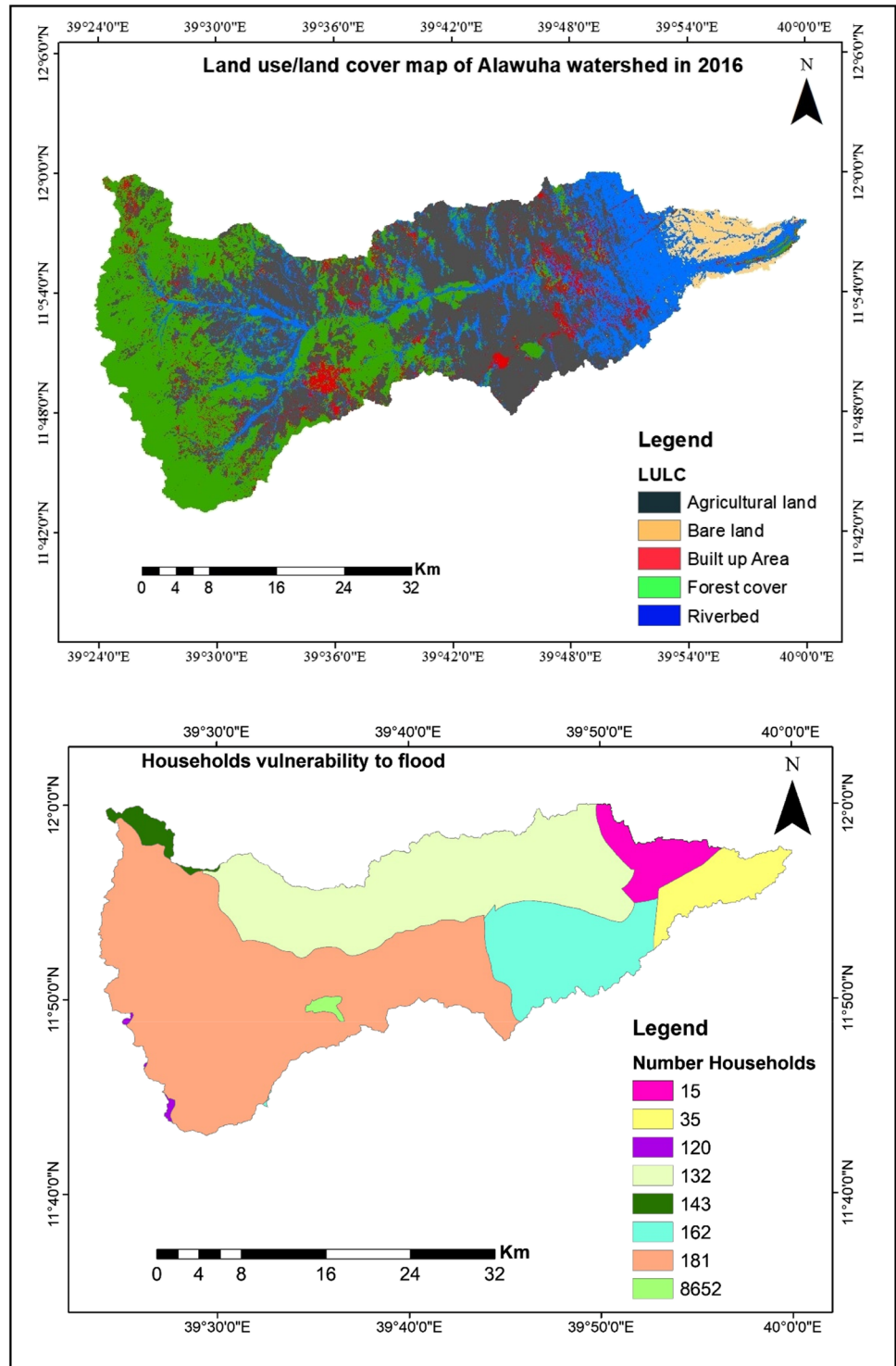
Fig. 9 Flood hazard map



of the study agrees with previous studies (Lin et al. 2020; Naif Rashed Alrehaili 2021; van der Sande et al. 2003). Agricultural land is also the second vulnerable land use class in the watershed because it is the primary economic activity of the country and the study area and the main

source of livelihood of the societies. The study confirmed a strong positive correlation between agriculture and flood vulnerability ($R^2 = 0.96$) and built-up and flood vulnerability ($R^2 = 0.93$).

Fig. 10 Households distribution and LULC map



Land use/land cover changes impact the condition for the change of precipitation into the spillover. Built-up impermeable regions cause the arrangement of a quick overland flow at the expense of the natural retention and subsurface or groundwater flow. There are a few bits of proof that adjustments of land use have impacted the hydrological system of different river basins. These effects can be huge in small

basins (Oda et al. 2021; Jones and Grant 1996). The hydrological effects of land use change depend not just on the general changes in land use types yet additionally on their spatial conveyance (Schumann et al. 2000). Besides, the change of agricultural, forest, grassland, and wetlands to urban regions generally accompanies a tremendous expansion in impenetrable surfaces, which can adjust the regular

Table 5 Correlation statistics of flood vulnerability and agricultural land

Summary output								
Regression statistics								
Multiple <i>R</i>	0.978654							
<i>R</i> square	0.957764							
Adjusted <i>R</i> square	0.915527							
Standard error	588.2177							
Observations	10							
ANOVA								
	<i>df</i>	<i>SS</i>	<i>MS</i>	<i>F</i>	<i>Significance F</i>			
Regression	1	7,845,997	7,845,997	22.67629	0.131774			
Residual	1	346,000.1	346,000.1					
Total	2	8,191,997						
	<i>Coefficients</i>	<i>Standard error</i>	<i>t Stat</i>	<i>P-value</i>	<i>Lower 95%</i>	<i>Upper 95%</i>	<i>Lower 95.0%</i>	<i>Upper 95.0%</i>
Flood event	30,158.56	3190.911	9.451396	0.067108	−10,385.8	70,702.92	−10,385.8	70,702.92
Agricultural land	−0.49355	0.103645	−4.76196	0.131774	−1.81049	0.82338	−1.81049	0.82338

hydrologic condition inside a watershed. It is surely known that the result of this change is ordinarily reflected in an expansion of the volume and pace of surface overflow and diminishes in groundwater re-energize and base flow (Dey and Mishra 2017; Moscrip and Montgomery 1997). This ultimately prompts bigger and more incessant occurrences of local flooding.

Flood and hydrology of a watershed show a close connection with the common land use. As the watershed turns out to be more evolved, it additionally turns out to be hydrologically more dynamic, changing the flood volume, overflow parts just as the beginning of streamflow. Nonetheless, floods that once happened rarely during predevelopment periods have now gotten more continuous and more extreme because of the change of watersheds starting with one land utilize then onto the next. Anthropogenic land use changes cause different hydrologic and geomorphic changes, including adjustments for the size and timing of flood peaks (Ricker et al. 2012; Miller et al. 1993) and in the size and kind of soil erosion (Zhu and Zhu 2011; Costa 1975). Then again, afforestation and the advancement of forest management will impressively expand the water maintenance in the landscapes (Marchi et al. 2018; Loyche Wilkie et al. 2003). Change in land use applies a critical impact on the relations of precipitation overflow and additionally spillover dregs (Li et al. 2019; Fu et al. 2002) and adjust soil and water trouble appropriately (Zheng and Wang 2013; Nemani et al. 2002). Recorded datasets of land use can be utilized to know the area and sorts of land use change as a stage towards examining the effect of such change on floods. Consequently, to moderate the flooding and catastrophe supportable flood, the board approach must be carried out because it has financial advantages like flood relief and ecological advantages like habitat reinstatement. This new worldview requires

a coordinated and comprehensive way to deal with flood management, which must be fused in both straightforwardly influenced regions and the whole basin or watershed. The consideration of the uplands and lowlands in the basin normally consolidates a wide scope of land utilizes, including forest, pasture, arable land, and urban regions. Thus, successful implementation of the sustainable flood management approach entails interdisciplinary coordination and participation at all levels of government, across different sectoral policies, and with all concerned stakeholders.

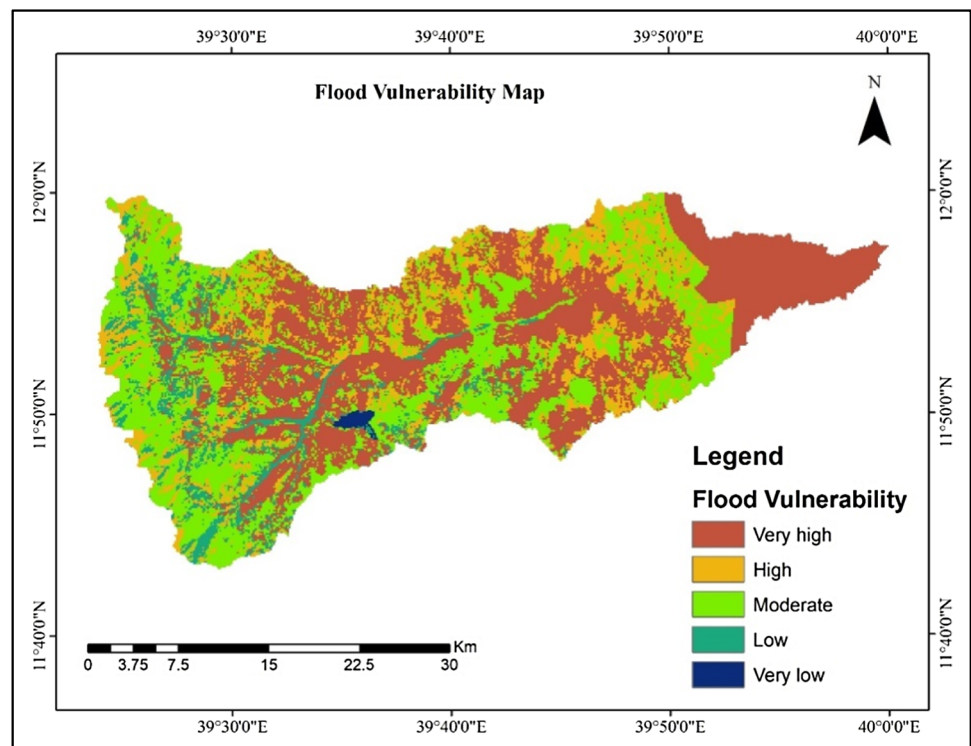
Flood risk indicators

The nature of the terrain and the direction of the slope affect the spatial variation of flooding and its risk. The result stated that steep slope terrain is more risk for flooding particularly when the land cover is altered and degraded. Rogger et al. (2017) found that when hill slopes are modified for agricultural production, there is a changing inflow path, flow velocities, water storage, and flow connectivity and concentration times. Moreover, the study confirmed an extreme agricultural land expansion worsens the risk of flooding mainly in highland area. On the other hand, the risk of flooding in lowland areas is commonly related to river peak flow, surface runoff, baseflow, and regression water from the larger water body (water accumulated areas). For instance, lowland areas of Dembia, Fogera, Dera, and Libo Kemkem districts were damaged due to peak flow water from the river and overflow water from Lake Tana. The study revealed that places found in downstream and lowland areas, as well as topographically steep slope places, have a high risk of flooding.

The type of slope coupled with the types of soil, rainfall amount, and elevation aggravating flood risk. They have impacts on flood generation, frequency, and magnitude of

Table 6 Correlation statistics of flood vulnerability and built-up area

Summary output								
Regression statistics								
Multiple <i>R</i>	0.962828							
<i>R</i> square	0.927037							
Adjusted <i>R</i> square	0.854074							
Standard error	773.119							
Observations	10							
ANOVA								
	<i>df</i>	<i>SS</i>	<i>MS</i>	<i>F</i>	<i>Significance F</i>			
Regression	1	7,594,284	7,594,284	12.70557	0.174125			
Residual	1	597,713	597,713					
Total	2	8,191,997						
	<i>Coefficients</i>	<i>Standard error</i>	<i>t Stat</i>	<i>P-value</i>	<i>Lower 95%</i>	<i>Upper 95%</i>	<i>Lower 95.0%</i>	<i>Upper 95.0%</i>
Flood event	9910.123	1509.438	6.56544	0.096226	−9269.1	29,089.35	−9269.1	29,089.35
Built-up	0.318801	0.089438	3.564487	0.174125	−0.81762	1.455219	−0.81762	1.455219

Fig. 11 Flood vulnerability map

floods. The result of this study indicates that Haplic Xerosols, Chromic Cambisols, Eutric Cambisols, and Vertic Cambisols have very high flooding capacity due to their low moisture availability and high porosity. Rogger et al. (2017) indicate that soil nature affects flow paths, including the type of runoff generation mechanism (overland flow versus subsurface storm flow). This study argues that slopes tend to reduce the amount of water infiltration into the ground; this water can then flow quickly down to rivers as overland flow mainly, steep slopes cause more through flow within

the soil. Moreover, elevation is used to determine flood insurance costs for high-risk zones (Samanta et al. 2018). The high potential of drainage density increases the possibility of flood risk since surface runoff and stream water overflow can be raised; particularly, the problem is severe during rainy seasons. Besides, drainage density increases in thickness from low values which will produce significant increases in the flood peaks (Pallard et al. 2009). Therefore, the study revealed that heavy and prolonged rainfall amount raises flood risk because it causes an increase of river water

Fig. 12 Flood risk map

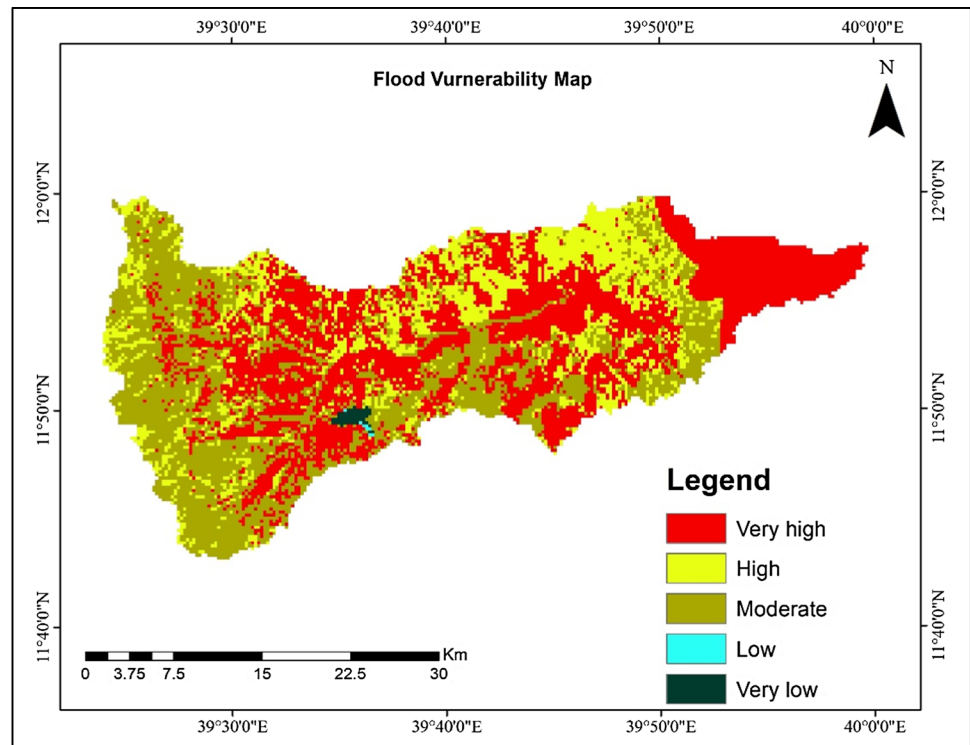


Table 7 Rainfall frequency analysis from 2000 to 2016

Year	Descending precipitation data in mm	Rank (i)	Annual exceedance probability (AEP)	Frequency or return period of an event (T)
2016	356.4	1	0.05	18.0
2012	313.8	2	0.13	7.5
2010	310.5	3	0.25	4
2015	306.9	4	0.23	4.25
2011	302.5	5	0.38	2.6
2002	296.8	6	1.49	0.67
2000	260.7	7	7.14	0.14
2003	241.2	8	1.61	0.62
2006	222.9	9	1.12	0.89
2007	220.7	10	1.11	0.9
2005	190.9	11	1.56	0.64
2001	181.4	12	4	0.25
2004	164.2	13	2.17	0.46
2009	159.2	14	1.26	0.79
2008	139.3	15	1.49	0.67
2013	125.9	16	1.06	0.94
2014	100.3	17	1.06	0.94

Source: Kombolcha Metrological Station, 2017

overflow from its channel and brings surface runoff. So, areas that are very close to the river are more at risk than others far from the river. Therefore, household’s property

and livelihood are more damaged when they are very close to the river and streams.

Causes of flood and management practices

Owing to its topographic and altitudinal characteristics, flooding is not new to Ethiopia (Shimeles and Woldemichael 2013). They have been occurring at different places and times with varying magnitude. A study also confirmed that flood disasters in South Omo and Dire Dawa city administration were an example of indicating flood occurrence severity in Ethiopia. Even though the cause of flooding will vary depending on the nature of the locality and the interventions that have been taken, intense rainfall is one of the main trigger factors of flooding mainly in the rainy season (Getahun and Gebre 2015).

The study area is characterized by rigid topography which makes it more to flooding especially for the communities around the riverside. The causes of flooding in the study area are improper tillage, slope terrain, deforestation, high seasonal rainfall, and the absence of protection measures. In addition, the increment of flooding is resulted from lack of agroforestry practices, farm terraces, homestead development, residue management, and free grazing. Weak awareness of local people towards soil and water conservation measures is also a contributing factor. The flooding events that happened from 2000 to 2016 have an effect on death, and displacement of peoples, and animals, crop loss, house destruction, topsoil removal, water pollution, and reduction of streamflow farmland fragmented and runoff increased, and more gullies and rills are created. Moreover, the 2016 flood event affected 9,440 households and caused the displacement of households from their location, injured, damage their economy, loss of property, livestock, and agriculture even though the severity of the risk varies spatially and temporally. Unless strong and sustainable flood management practice measures are taken, the study confirms that the area will be affected by flood disasters like the 2016 flood with a return period of 18 years with a 0.05 probability of occurrence.

To minimize the problems of flooding in the study area, various soil and water conservation practices were performed in the watershed including terraces, ditch trenches, contour ploughing, stone bunds, check dams, soil bunds, and others. However, implementations of these soil and water conservation practices do not follow any scientific approaches. According to field observation made in the watershed, the farmland in dry areas has fewer agroforestry practices with predominately covered by cereal crops, but Dega parts of the watershed have relatively more agroforestry practices. Eucalyptus is the most common tree found in the upper watershed. Few farmers in the upper parts of the watershed use local stone bunds to avoid excess runoff. Some farmers use traditional soil bund in their farmland. Most soil and water conservation activities are introduced by the Woreda agriculture office through its regular agricultural

extension services and productive safety net programs and other supporting organizations. High cost of construction and labor shortage are challenges of efficient implementation of flood control mechanisms practiced due to the high cost of construction and high labor demanding.

Conclusions

Flood disaster management can be effective only when thorough information is acquired about the expected frequency, character, and magnitude of hazardous events in an area and the vulnerabilities of the people, buildings, infrastructure, and economic activities in potentially dangerous areas. In this investigation, various parameters were identified as flood aggravating factors with different hazard values such as slope, elevation, soil type, drainage density, distance from streams, and rainfall amount. These flood aggravating factors result in flood vulnerability on people, land uses, land cover, and other elements like infrastructures and economic activities. The main causes of flooding in the catchment area are improper tillage, slope terrain, deforestation, high seasonal rainfall, and absence of protection measures. These problems result in a decrease or dry stream flow, farmland fragmentation, increase runoff, creation of gullies and rills, death of cattle, crop and infrastructure destruction, a decline in soil fertility, and pollution of water bodies as well as the death of people. The GIS multi-criteria evaluation of flood risk assessment shows the area under the highly vulnerable in the watershed. Therefore, for those areas, different watershed conservation measures were taken by the stakeholder to minimize the flood's physical and biological risks in the Alawuha watershed even though their effectiveness is under question.

To effectively adopt various biological and physical measures for flood management in the watershed, the local government authorities are responsible for creating awareness about the high probability of flood occurrences and their risk in the area. The local disaster risk management and food security offices must install flood hazard indicator technology in high flood risk areas to alarm the people who live in the room when flooding occurs. Besides, based on the nature and extent of degradation as well as the purpose of conservation, different soil and water conservation (SWC) measures will be identified. This may include physical or structural measures, biological (vegetative) measures, agronomic (best management practices) measures, or area closure. Physical measures are structures built for soil and water conservation. They are built with the principle to (1) increase the time of concentration of runoff, thereby allowing more of it to infiltrate into the soil; (2) divide a long slope into several short ones and

thereby reduce the amount and velocity of surface runoff; (3) reduce the velocity of the surface runoff; and (4) protect against damage due to excessive runoff. Moreover, biological measures of soil and water conservation provide a protective impact through vegetation cover. Vegetation cover has the functions of (i) preventing splash erosion, (ii) reducing the velocity of surface runoff, (iii) facilitating the accumulation of soil particles, (iv) increasing surface roughness which reduces runoff and increases infiltration, and (v) stabilizing soil aggregates through their roots and organic matter which in turn increase infiltration. Thus, watershed conservation practices must be conducted based on the hydrological unit rather than the administrative unit.

Author contribution The authors prepared the research proposal; collected, encoded, and interpreted the spatial data; and wrote the research report draft. They processed and derived LULC classes from Landsat images, analyzed and interpreted flood modeling, and prepared the manuscript for publication. The authors edited and revised the manuscript and approved it to send to the journal.

Data availability All data generated or analyzed during this study are included in this published article [and its supplementary information files].

Declarations

Ethics approval and consent to participate Not applicable.

Consent for publication Not applicable.

Competing interests The authors declare no competing interests.

Author information Fisha Semaw and Abel Balew graduated in Geography and Environmental Studies from Mada walabu University and gained their MSc degree in GIS and Remote Sensing from Addis Ababa University. Getnet Zeleke graduated in Geography and Environmental Studies from Wollega University and gained his MSc degree in Environmental Management from Addis Ababa University. Currently, the authors are working as a lecturer in Woldia University.

References

- Akola J, Binala J, Ochwo J (2019) Guiding developments in flood-prone areas: challenges and opportunities in Dire Dawa city, Ethiopia. *Jamba J Disaster Risk Stud* 11(3). <https://doi.org/10.4102/jamba.v11i3.704>
- Alemu W, Legesse Belachew D (2011). Flood hazard and risk assessment using GIS and remote sensing in Fogera Woreda, Northwest Ethiopia. https://doi.org/10.1007/978-94-007-0689-7_9
- Ali SY (2002) Small-scale irrigation and household food security: a case study of three irrigation schemes in Gubalافت Woreda of North Wollo zone, Amhara region. Dissertation, Addis Ababa University
- Assegid E (2007) Suitability analysis of the proposed upland rice production using GIS and remote sensing in Fogera Woreda. Addis Ababa University, Thesis
- Barasa BN, Perera EDP (2018) Analysis of land use change impacts on flash flood occurrences in the Sosiani River basin Kenya. *Int J River Basin Manag* 16(2):179–188
- Bhatt, G., Kumar, M., & Duffy, C. J (2014) A tightly coupled GIS and distributed hydrologic modeling framework. *Environ Model Softw* 62: 70–84. <https://doi.org/10.1016/j.envsoft.2014.08.003>
- Bishaw, K (2012) Application of GIS and remote sensing techniques for flood hazard and risk assessment. Thesis, Ethiopian Civil Service University
- Boudiaf B, Dabanli I, Boutaghane H, Şen Z (2020) Temperature and precipitation risk assessment under climate change effect in north-east Algeria. *Earth Syst Environ* 4:1–14. <https://doi.org/10.1007/s41748-019-00136-7>
- Cao C, Xu P, Wang Y, Chen J, Zheng L, Niu C (2016) Flash flood hazard susceptibility mapping using frequency ratio and statistical index methods in coalmine subsidence areas. *Sustainability* 8(9):948
- Chen YR, Yeh CH, Yu B (2011) Integrated application of the analytic hierarchy process and the geographic information system for flood risk assessment and flood plain management in Taiwan. *Nat Hazards* 59(3):1261–1276
- Chikoto GL, Sadiq A, Fordyce E (2013) Disaster mitigation and preparedness. *Nonprofit Volunt Sect Q* 42:391–410
- Congalton RG, Green K (2008) Assessing the accuracy of remotely sensed data: principles and practices, Second Edition (2nd ed.). CRC Press. <https://doi.org/10.1201/9781420055139>
- Costa JE (1975) Effects of agriculture on erosion and sedimentation in the Piedmont Province, Maryland. *Geol Soc Am Bull* 86(9):1281–1286
- Danumah JH, Odai SN, Saley BM, Szarzynski J, Thiel M, Kwaku A, Akpa LY (2016) Flood risk assessment and mapping in Abidjan district using multi-criteria analysis (AHP) model and geoinformation techniques, (cote d’ivoire). *Geoenviron Dis* 3(10):1–13. <https://doi.org/10.1186/s40677-016-0044-y>
- Darama Y, Seyrek K (2016) Determination of watershed boundaries in Turkey by GIS based hydrological river basin coding. *J Water Resour Prot* 8:965–981. <https://doi.org/10.4236/jwarp.2016.811078>
- Desalegn H, Mulu A (2021) Flood vulnerability assessment using GIS at Fetam watershed, upper Abbay basin. Ethiopia. *Heliyon* 7(1):e05865
- De Risi R, Jalayer F, De Paola F et al (2020) From flood risk mapping toward reducing vulnerability: the case of Addis Ababa. *Nat Hazards* 100:387–415. <https://doi.org/10.1007/s11069-019-03817-8>
- Dennis Mileti (1999) *Disasters by design: a reassessment of natural hazards in the United States*. Washington, DC: Joseph Henry Press. <https://doi.org/10.17226/5782>.
- Dey P, Mishra A (2017) Separating the impacts of climate change and human activities on streamflow: a review of methodologies and critical assumptions. *J Hydrol* 548. <https://doi.org/10.1016/j.jhydrol.2017.03.014>.
- El Bastawesy M, White K, Nasr A (2009) Integration of remote sensing and GIS for modelling flash floods in Wadi Hudain catchment, Egypt. *Hydrol Process* 23(9):1359–1368
- Eleni, K., Ioannis, F., Alexandros, K., Emmanouil, A., Konstantinos, N (2011) Flood hazard assessment based on geomorphological analysis with GIS tools—the case of Laconia (Peloponnesus, Greece). In: *Proceedings of Symposium GIS Ostrava 24–26 January 2011*
- Elkhrachy I (2015) Flash flood hazard mapping using satellite images and GIS tools: a case study of Najran City, Kingdom of Saudi Arabia (KSA). *Egypt J Remote Sens Space Sci* 18(2):261–278
- Fan F, Wang Y, Qiu M, Wang Z (2009) Evaluating the temporal and spatial urban expansion patterns of Guangzhou from 1979 to 2003 by remote sensing and GIS methods. *Int J Geogr Inf Sci* 23(11):1371–1388

- Feloni E, Mousadis I, Baltas E (2020) Flood vulnerability assessment using a GIS-based multi-criteria approach: the case of Attica region. *J Flood Risk Manag* 13:e12563
- Fu B, Qiu Y, Wang J, Chen L (2002) Effect simulations of land use change on the runoff and erosion for a gully catchment of the Loess Plateau. *China ACTA Geographica Sinica-Chinese Edition* 57(6):717–722
- Getahun YS, Gebre SL (2015) Flood hazard assessment and mapping of flood inundation area of the Awash River Basin in Ethiopia using GIS and HEC-GeoRAS/HEC-RAS model. *J Civ Environ Eng* 5(4):1
- Ghani AA, Ali R, Zakaria NA, Hasan ZA, Chang CK, Ahamad MSS (2010) A temporal change study of the Muda River system over 22 years. *Int J River Basin Manag* 8(1):25–37
- Hadjimitsis DG (2010) Brief communication “Determination of urban growth in catchment areas in Cyprus using multi-temporal remotely sensed data: risk assessment study.” *Nat Hazard* 10(11):2235–2240. <https://doi.org/10.5194/nhess-10-2235-2010>
- Horton RE (1945) Erosional development of streams and their drainage basins; hydrophysical approach to quantitative morphology. *Geol Soc Am Bull* 56(3):275–370
- ISDR, U.N (2009) Global assessment report on disaster risk reduction. United Nations International Strategy for Disaster Reduction (UN ISDR), Geneva, Switzerland, ISSN, 980852698, 207
- Jiang J, Tian G (2010) Analysis of the impact of land use/land cover change on land surface temperature with remote sensing. *Procedia Environ Sci* 2:571–575
- Jones JA, Grant GE (1996) Peak flow responses to clear-cutting and roads in small and large basins, western Cascades, Oregon. *Water Resour Res* 32(4):959–974
- Kazakis N, Kougiaris I, Patsialis T (2015) Assessment of flood hazard areas at a regional scale using an index-based approach and analytical hierarchy process: application in Rhodope-Evros region, Greece. *Sci Total Environ* 538:555–563. <https://doi.org/10.1016/j.scitotenv.2015.08.055>
- Kia MB, Pirasteh S, Pradhan B, Mahmud AR, Sulaiman WNA, Moradi A (2012) An artificial neural network model for flood simulation using GIS: Johor River Basin. *Malaysia Environ Earth Sci* 67(1):251–264
- Kim J, Scott CD (2012) Robust kernel density estimation. *The J Mach Learn Res* 13(1):2529–2565
- Kusmiyarti TB, Wiguna PPK, Dewi NR (2018) Flood risk analysis in Denpasar City, Bali, Indonesia. In: Proceedings of IOP Conference Series: Earth and Environmental Science 123(1): 012012. IOP Publishing. <https://doi.org/10.1088/1755-1315/123/1/012012>
- Lee MJ, Kang JE, Jeon S (2012) Application of frequency ratio model and validation for predictive flooded area susceptibility mapping using GIS. In: proceedings of 2012 IEEE international geoscience and remote sensing symposium, pp. 895–898
- Lincoln WS, Zogg J, Brewster J (2016) Addition of a vulnerability component to the flash flood potential index. https://www.weather.gov/media/lmrfc/tech/2016_Vulnerability_Component_FFPI.pdf
- Li S, Liu X, Li Z, Wu Z, Yan Z, Chen Y, Gao F (2018) Spatial and temporal dynamics of urban expansion along the Guangzhou-Foshan Inter-City Rail Transit Corridor, China
- Li Y, Li Y, Fan P, Sun J, Liu Y (2019) Land use and landscape change driven by gully land consolidation project: a case study of a typical watershed in the Loess Plateau. *J Geog Sci* 29(5):719–729. <https://doi.org/10.1007/s11442-019-1623-0>
- Lin Y-T, Yang M-D, Han J-Y, Su Y-F, Jang J-H (2020) Quantifying flood water levels using image-based volunteered geographic information. *Remote Sensing* 12(4):706. <https://doi.org/10.3390/rs12040706>
- Loakes KL, Ryves DB, Lamb HF, Schäbitz F, Dee M, Tyler JJ, McGowan S (2018) Late quaternary climate change in the north-eastern highlands of Ethiopia: a high resolution 15,600 year diatom and pigment record from Lake Hayk. *Quatern Sci Rev* 202:166–181. <https://doi.org/10.1016/j.quascirev.2018.09.005>
- Loyche Wilkie M, Holmgren P, Castaneda F (2003) Sustainable forest management and the ecosystem approach: two concepts, one goal
- Marchi E, Chung W, Visser R, Abbas D, Nordfjell T, Mederski PS, Mcewan A, Brink M, Laschi A (2018) Sustainable forest operations (SFO): a new paradigm in a changing world and climate. *Sci Total Environ* 634:1385–1397
- Mengistie D, Kidane D (2016) Assessment of the impact of small-scale irrigation on household livelihood improvement at Gubalafto District, North Wollo, Ethiopia. *Agriculture* 6:1–22
- Miller SO, Ritter DF, Kochel RC, Miller JR (1993) Fluvial responses to land-use changes and climatic variations within the Drury Creek watershed, southern Illinois. *Geomorphology* 6(4):309–329
- Moscip AL, Montgomery DR (1997) Urbanization, flood frequency, and salmon abundance in Puget lowland streams. *J Am Water Resour Assoc* 33(6):1289–1297
- Nachtergaele F, van Velthuisen H, Verelst L, Batjes NH, Dijkshoorn K, van Engelen VWP, ... , Montanarella L (2010) The harmonized world soil database. In: Proceedings of the 19th World Congress of Soil Science, Soil Solutions for a Changing World, Brisbane, Australia, 1–6 August 2010, pp. 34–37
- Naif Rashed Alrehaili (2021) A systematic review of the emergency planning for flash floods response in the Kingdom of Saudi Arabia: Australian Institute for Disaster Resilience 82–88. <https://doi.org/10.47389/36.4.82>
- Nemani R, White M, Thornton P, Nishida K, Reddy S, Jenkins J, Running S (2002) Recent trends in hydrologic balance have enhanced the terrestrial carbon sink in the United States. *Geophys Res Lett* 29(10):106–111
- Niyongabire E, Hassan R, Elhassan E, Mehdi M (2016) Use of digital elevation model in a GIS for flood susceptibility mapping: case of Bujumbura City. In: Proceedings of 6th international conference on cartography and GIS, Albena: Bulgaria, pp. 241–248
- Nkeki FN, Henah PJ, Ojeh VN (2013) Geospatial techniques for the assessment and analysis of flood risk along the Niger-Benue Basin in Nigeria. *J Geogr Inf Sci* 5(2):123–135. <https://doi.org/10.4236/jgis.2013.5.2013>
- Oda T, Egusa T, Ohte N, Hotta N, Tanaka N, Green M, Suzuki M (2021) Effects of changes in canopy interception on stream runoff response and recovery following clear-cutting of a Japanese coniferous forest in Fukuroyamasawa Experimental Watershed in Japan. *Hydrol Process.* 35. <https://doi.org/10.1002/hyp.14177>
- Ogarekpe NM, Obio EA, Tenebe IT, Emenike PC, Nnaji CC (2020) Flood vulnerability assessment of the upper Cross River basin using morphometric analysis. *Geomat Nat Haz Risk* 11(1):1378–1403
- Ologunorisa TE (2004) An assessment of flood vulnerability zones in the Niger Delta, Nigeria. *Int J Environ Stud* 61(1):31–38. <https://doi.org/10.1080/0020723032000130061>
- Ouma YO, Tateishi R (2014) Urban flood vulnerability and risk mapping using integrated multi-parametric AHP and GIS: methodological overview and case study assessment. *Water* 6(6):1515–1545
- Pallard B, Castellarin A, Montanari A (2009) A look at the links between drainage density and flood statistics. *Hydrol Earth Syst Sci* 13(7):1019–1029. <https://doi.org/10.5194/hess-13-1019-2009>
- Papaoannou G, Vasiliades L, Loukas A (2015) Multi-criteria analysis framework for potential flood prone areas mapping. *Water resources management* 29(2):399–418

- Rahmati O, Pourghasemi HR, Zeinivand H (2016) Flood susceptibility mapping using frequency ratio and weights-of-evidence models in the Golastan Province. *Iran Geocarto International* 31(1):42–70
- Ricker MC, Donohue SW, Stolt MH, Zavada MS (2012) Development and application of multi-proxy indices of land use change for riparian soils in southern New England, USA. *Ecological Applications*, 22(2), 487–501. <http://www.jstor.org/stable/41416777>.
- Rimba AB, Setiawati MD, Sambah AB, Miura F (2017) Physical flood vulnerability mapping applying geospatial techniques in Okazaki City, Aichi Prefecture. *Japan Urban Science* 1(1):7
- Rogger M, Agnoletti M, Alaoui A, Bathurst JC, Bodner G, Borga M, Blöschl G (2017) Land use change impacts on floods at the catchment scale: challenges and opportunities for future research. *Water Resour Res* 53(7):5209–5219
- Samanta RK, Bhunia GS, Shit PK, Pourghasemi HR (2018) Flood susceptibility mapping using geospatial frequency ratio technique: a case study of Subarnarekha River Basin. *India Modeling Earth Systems and Environment* 4(1):395–408. <https://doi.org/10.1007/s40808-018-0427-z>
- Sarkar D, Mondal P (2020) Flood vulnerability mapping using frequency ratio (FR) model: a case study on Kulik river basin. *Indo-Bangladesh Barind Region Applied Water Science* 10(1):1–13
- Schumann AH, Funke R, Schultz GA (2000) Application of a geographic information system for conceptual rainfall–runoff modeling. *J Hydrol* 240(1–2):45–61
- Sena L and Michael KW (2006) Disaster prevention and preparedness. Ethiopia Public Heal Train Initiat 1: 1–80. Thesis, Addis Ababa University
- Shaaban F, Othman A, Habeebullah T, Saoud W (2021) An integrated GPR and geoinformatics approach for assessing potential risks of flash floods on high-voltage towers, Makkah. *Saudi Arabia Environmental Earth Sciences* 80:199. <https://doi.org/10.1007/s12665-021-09454-4>
- Shimeles A, Woldemichael A (2013) Rising food prices and household welfare in Ethiopia: evidence from micro data. African Development Bank Group, Working Paper Series (182)
- Singh G, Pandey A (2021) Flash flood vulnerability assessment and zonation through an integrated approach in the Upper Ganga Basin of the Northwest Himalayan region in Uttarakhand. *International Journal of Disaster Risk Reduction* 66:102573. <https://doi.org/10.1016/j.ijdrr.2021.102573>
- Tehrany MS, Pradhan B, Jebur MN (2013) Spatial prediction of flood susceptible areas using rule based decision tree (DT) and a novel ensemble bivariate and multivariate statistical models in GIS. *J Hydrol* 504:69–79
- Tehrany MS, Pradhan B, Jebur MN (2014) Flood susceptibility mapping using a novel ensemble weights-of-evidence and support vector machine models in GIS. *J Hydrol* 512:332–343
- Tehrany MS, Pradhan B, Jebur MN (2015) Flood susceptibility analysis and its verification using a novel ensemble support vector machine and frequency ratio method. *Stoch Env Res Risk Assess* 29(4):1149–1165
- Trenberth KE (2008) The impact of climate change and variability on heavy precipitation, floods, and droughts. *Encyclopedia of Hydrological Sciences*. <https://doi.org/10.1002/0470848944.hsa211>
- Van der Sande CJ, De Jong SM, De Roo APJ (2003) A segmentation and classification approach of IKONOS-2 imagery for land cover mapping to assist flood risk and flood damage assessment. *Int J Appl Earth Obs Geoinf* 4(3):217–229
- Weibull W (1939) A statistical theory of the strength of material. *R. Swedish Acad. Eng. Sci. Proc.* No 151:1–45
- Weldegebriel ZB, Amphune BE (2017) Livelihood resilience in the face of recurring floods: an empirical evidence from Northwest Ethiopia. *Geoenvironmental Disasters* 4(10):1–19. <https://doi.org/10.1186/s40677-017-0074-0>
- Wu H, Gu G, Yan Y, Gao Z, Adler RF (2018) Global flood monitoring using satellite precipitation and hydrological modeling. *Global Flood Hazard: Applications in Modeling, Mapping, and Forecasting* 87-113. <https://doi.org/10.1002/9781119217886.ch6>
- Xiong J, Li J, Cheng W, Wang N, Guo L (2019) A GIS-based support vector machine model for flash flood vulnerability assessment and mapping in China. *ISPRS Int J Geo Inf* 8(7):297
- Zachariev G (2016) A statistical theory of the damage of materials. *Modern Mechanical Engineering* 6:129–150. <https://doi.org/10.4236/mme.2016.64013>
- Zheng C, Wang Q (2013) Spatiotemporal variations of reference evapotranspiration in recent five decades in the arid land of Northwestern China. *Hydrol Process* 28(25):6124–6134. <https://doi.org/10.1002/hyp.10109>
- Zhu L, Zhu W (2011) Study on soil erosion and its effects on agriculture sustainable development in west Henan province loess hilly areas. 2011 International Symposium on Water Resource and Environmental Protection. <https://doi.org/10.1109/iswrep.2011.5893593>.